Pergamon

Int. J. Multiphase Flow Vol. 23, No. 5, pp. 845–863, 1997

Printed in Great Britain
PII: S0301-9322(97)00007-4
0301-9322/97 $17.00 + 0.00

LIQUID-TO-WALL SHEAR STRESS DISTRIBUTION IN STRATIFIED/ATOMIZATION FLOW

N. A. VLACHOS, S. V. PARAS and A. J. KARABELAS

Department of Chemical Engineering and Chemical Process Engineering Research Institute, Aristotle University of Thessaloniki, University Box 455, GR 540 06 Thessaloniki, Greece

(Received 15 August 1996; in revised form 20 February 1997)

Abstract—Experiments were conducted in a horizontal flow loop (24 mm i.d.), using an electrochemical technique, for measuring liquid-to-wall shear stress, at various positions around the pipe circumference. Measurements of liquid film thickness, pressure drop as well as visual observations were also made. These data complement similar information obtained by Paras *et al.* (1994), in a horizontal 50.8 mm i.d. flow system. Mean values and other statistical information are obtained from the analysis of the shear stress and film thickness data. Visual studies of the gas/liquid interface confirm that its profile is concave rather than flat. The data show that the time-averaged shear stress tends to decrease in the lateral direction (i.e. away from the pipe bottom, $\Theta = 0°$) along which the liquid film gradually becomes thinner. Only for relatively low superficial gas velocities (e.g. $U_G < 15$ m/s), the mean shear stress is almost constant up to $\Theta = 45°$; i.e. in a flow region where there is a relatively thick liquid layer. An expression is proposed for predicting the shear stress circumferential distribution. By means of momentum balances (utilizing the new data), the average gas/liquid interfacial friction factor is determined with improved accuracy. Additionally an equivalent gas/liquid interface roughness is expressed in terms of wave characteristics, i.e. wave intermittency and amplitude. © 1997 Elsevier Science Ltd.

Key Words: stratified/atomization flow, gas/liquid flow, electrochemical technique, liquid-to-wall shear stress

1. INTRODUCTION

The stratified/atomization flow regime is frequently encountered in various industrial processes; e.g. steam and water pipe flow, natural gas and oil transfer pipelines etc. To handle practical problems such as prediction of friction losses or determination of corrosion and scaling rates, it is necessary to gain a better understanding of flow characteristics and of the transport phenomena in this particular flow regime. Aside from its practical significance, stratified/atomization flow is considered quite significant from the research standpoint. Indeed, this regime shares the same basic features (wavy liquid layer at the pipe bottom, droplet atomization caused by the fast moving gas) with the (neighbouring) horizontal annular flow regime that prevails at higher gas flow rates. It is clear, however, that the stratified/atomization regime is simpler and more convenient to study than the more complicated annular flow.

On the basis of these ideas, an effort has been undertaken in this laboratory to systematically study stratified/atomization flow. A 50.8 mm i.d. flow loop was initially employed in the tests. Paras and Karabelas (1992) made local (non-intrusive) LDA velocity measurements inside the *liquid layer* at the pipe bottom. Significant information was obtained concerning the flow structure of the turbulently flowing liquid. Similar (LDA) techniques were recently used by Paras *et al.* (1996) to measure the local velocity distribution in the *gas phase*. The existence of secondary flow currents and the strong influence of the wavy gas/liquid interface (on the gas flow field) was evident in these data.

In another study Paras *et al.* (1994) obtained fairly complete sets of film thickness data and offered an improved picture of liquid layer characteristics, including the gas/liquid interface shape and friction factor. Limited shear stress measurements were also reported, using hot-film probes flush mounted at $\Theta = 0°$ and 45° from the pipe bottom. These data strongly suggested that there was a very uneven liquid-to-wall circumferential shear stress (τ_{wL}) distribution. This was contrary

to the recommendations or assumptions usually made in the literature (e.g. Agrawal *et al.* 1973; Taitel and Dukler 1976; Fisher and Pearce 1979) that τ_{wL} is nearly uniform. Therefore, it was necessary to clarify this issue by making detailed measurements of liquid-to-wall shear stress, at various positions around the pipe circumference.

A well-known electrochemical (or electro-diffusion) technique is employed in this study, with circular electrodes (0.5 mm dia.) embedded in the pipe wall. This technique has been used repeatedly with circular wall electrodes (e.g. Reiss and Hanratty 1962; Jolls and Hanratty 1969; Karabelas *et al.* 1973). The small circular probes have an advantage over hot-film sensors in that they can be closely spaced in the pipe circumference. Thus, 11 such electrodes were flush mounted over the pipe circumference in the present experiments.

More recently, the electrochemical method was employed for wall shear stress measurements by Nakoryakov *et al.* (1981), Cognet *et al.* (1984) and Zabaras (1985) in vertical gas/liquid two-phase flows, in pipes of internal diameter 86.4, 44 and 50.8 mm respectively, by Sobolík *et al.* (1987) in flows of non-Newtonian liquids in wavy vertical films and by Rode *et al.* (1994) in measurements of liquid flow in packed beds. Platinum wall microelectrodes of 0.5 mm diameter distributed circumferentially in a 19 and 82 mm i.d. pipe, were employed by Krokovny *et al.* (1973) and Rosant (1993), respectively, for measuring liquid-to-wall shear stress in horizontal (or near horizontal) gas/liquid flow.

Flush-mounted hot film probes were employed by Kowalski (1987) to measure wall stress τ_{wL}. Shear stress measurements of some relevance to this work were also reported by Hagiwara *et al.* (1989), for horizontal wavy two-phase flow as well as by Miya *et al.* (1971) and McCready and Hanratty (1985) in a rectangular channel using hot film probes.

In this paper the new experimental set-up is described first. The results follow, where shear stress measurements are complemented with new film thickness and pressure drop data. Visual observations are included to estimate the fraction of pipe circumference wetted by the liquid. The data are interpreted and correlated, including expressions for space-averaged τ_{wL} and gas/liquid friction factor.

2. EXPERIMENTAL SETUP AND TECHNIQUES

The experiments were carried out near atmospheric pressure, in a newly constructed *horizontal* flow loop, where two-phase flow developed in a 24 mm i.d. Plexiglas tube with a 5 m long straight

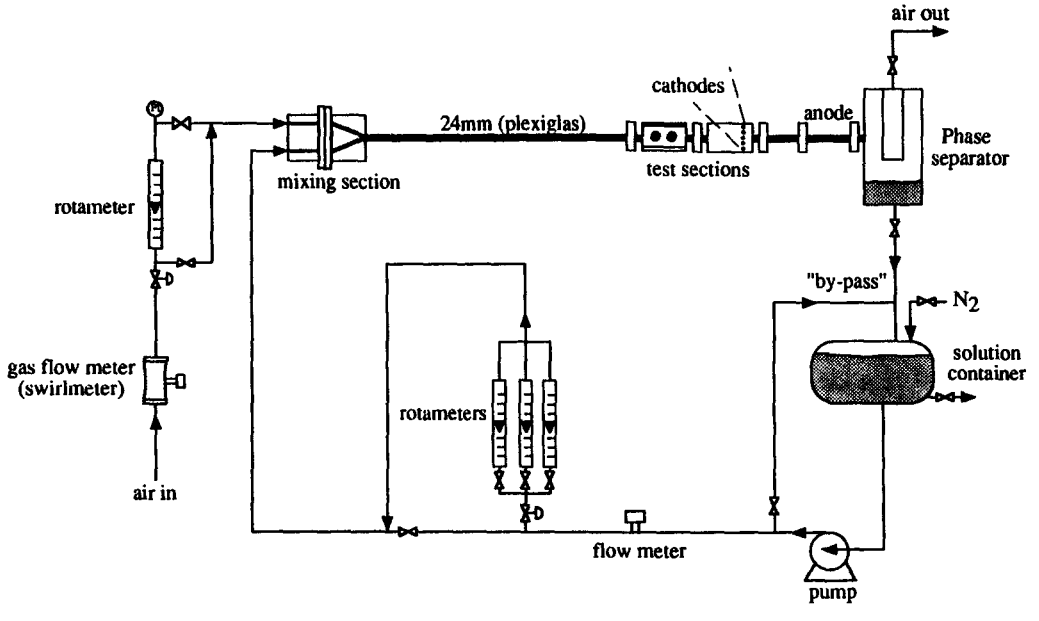

Figure 1. Schematic layout of the flow loop.

section. A schematic layout of the flow loop is shown in figure 1. This setup is of smaller scale than an existing 50.8 mm i.d. pipe loop in order to better control the conditions of the electrochemical system and to reduce the volume of the photo-sensitive liquid inventory, thus ensuring constant liquid properties.

The liquid flow rate is measured using a set of three rotameters together with a low-flow paddle-wheel sensor. The electrochemical solution is collected in a 70 l storage tank and is recirculated through the loop by means of a centrifugal chemical pump. Properly conditioned air (filtered, dried) is supplied to the rig and its flow rate is measured by means of a calibrated rotameter and by a swirlmeter (used for relatively high air velocities). The superficial velocities are varied in the range $U_L = 1$–5 cm/s for the liquid (electrochemical solution) and $U_G = 10$–25 m/s for the air, where stratified/atomization flow regime is developed.

Two specially designed test sections are positioned approximately 4 m away from the mixing section of the two phases. The first (upstream) test section is designed to accommodate parallel wire conductance probes together with flush-mounted hot-film probes for measuring instantaneous film thickness and wall shear stress respectively, at the pipe bottom. The conductance probes have two long parallel chromel wires 0.3 mm in diameter and 2 mm apart, covering the entire pipe diameter. The probes are part of an electronic circuit, comprised of a custom-made analyzer and a function generator with a 25 kHz carrier signal. Conductivity measurements of the electrochemical solution were made prior to and after each run, for eliminating the temperature effect on the wire probe conductance. A calibrated (in single phase flow) flush-mounted hot-film probe (DANTEC 55R46) was used for performing only limited liquid-to-wall shear stress measurements, for comparison with the electrochemical technique mainly employed in this work. There was quite a satisfactory agreement (deviation 5–10%) between the two methods. The parallel wire conductance probe technique and the flush-mounted hot-film probes are described in more detail elsewhere (Paras *et al.* 1994).

The second (downstream) test section was designed exclusively for shear stress measurements using the limiting current (or electro-diffusion) technique. In this electrochemical method, the diffusion limiting current which results from the transfer of ions to a small electrode (cathode), is controlled by hydrodynamic conditions. At high enough voltages the working electrodes are polarized, so that the reaction rate is fast and the process is controlled by the liquid-to-solid mass transfer rate. The space-averaged mass transfer coefficient is computed directly from the measured diffusional current and it is related to the local wall shear stress, at the surface of the probe (Reiss and Hanratty 1962). A rather detailed review of this technique is presented by Selman and Tobias (1978).

A fluid mixture of potassium ferricyanide (0.01 M) and potassium ferrocyanide (0.05 M), with sodium hydroxide (1 M) acting as neutral electrolyte, was used. The same composition of the electrolytic solution was used by Tsochatzidis and Karabelas (1994) for measuring local liquid–solid mass transfer coefficients. The measured density of the solution was 1053 Kg/m^3 whereas the viscosity was 1.3×10^{-3} Kg/(ms) at 20°C. The latter was corrected for changes in temperature. The ferricyanide diffusivity was obtained by an equation proposed by Gordon *et al.* (1966). The solution was titrated prior to and after the experiments (with a procedure described in Vogel 1962) to determine the exact bulk concentration of the ferricyanide ions. During the experiments the solution in the tank was preserved in a nitrogen atmosphere, for protection from dissolved oxygen, whereas the Plexiglas tube was covered by aluminum foil to protect the photo-sensitive electrolytic solution from light exposure. The latter has to be discarded after a relatively short period of time (i.e. every 2–3 weeks).

The special test section is instrumented with 10 isolated circular electrodes embedded (flush with the inner surface) around the pipe circumference, at $\Delta\Theta = 22.5°$ intervals (electrodes #1 to #9), from the pipe bottom (at 0°) to the pipe top (at 180°), all located at one pipe cross section (figure 2). Electrode #10 is positioned at 315° (at the same cross section) i.e. symmetrically with the electrode #3, which is placed at 45°. At another cross-section of the pipe, located 2 cm upstream from the first, electrode #11 is positioned at 45°. Each small electrode, made of nickel wire 0.5 mm in diameter, is mounted flush with the tube wall and very carefully polished. A thin nickel sheet (of 0.125 mm thickness), glued onto the tube inner surface, with a much greater surface area ($\sim$30 cm long), acts as the anode, located about 30 cm downstream of the cathodes (small

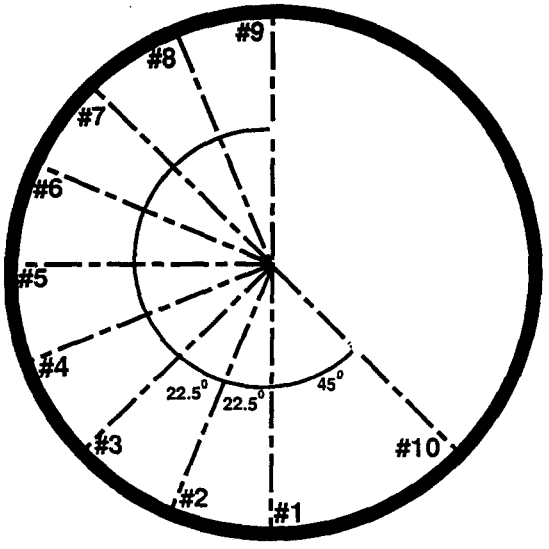

Figure 2. Distribution of electrodes around the pipe circumference.

electrodes). The wall electrodes have to be calibrated in situ, in horizontal single-phase flow, to account mainly for imperfections of their exposed surface. The calibration is carried out for each electrode prior to and after the main experiments.

Pressure drop measurements are carried out using an electronic differential pressure transmitter connected to two pressure taps. These taps are 3 m apart and located at the pipe bottom. Special care is taken to purge, from air bubbles, the lines connecting the transmitter. Also visual observations are made with an angle gauge, for measuring the angle θ (wetted wall fraction) over which the pipe walls are wetted by the liquid phase.

The diffusion limiting current (of each cathode separately) is converted to voltage (by means of precision resistances), amplified, fed to a 12 bit A/D converter and stored in a PC 486 compatible, using a computer code developed in this laboratory. The analog output from the analyzer and the hot film probe unit are also digitized and recorded by the computer. Data sets of liquid-to-wall shear stress and film thickness are collected for a period of ~ 16.5 s with a sampling frequency of 500 Hz.

3. RESULTS

The flow conditions for all runs are summarized in table 1. Time-averaged liquid-to-wall shear stress data, at various locations around the pipe circumference, together with film thickness data, at the pipe bottom, two-phase pressure drop data and values of wetted wall fraction are also included in this table. All data were obtained in the stratified/atomization flow regime, except a few taken in the annular regime; i.e. runs O, Q and R.

3.1. Film thickness

Statistical analysis of film records at the pipe bottom ($\Theta = 0°$) has allowed the study of variation of time-averaged thickness and of RMS values. As one might have expected, the mean film thickness increases with liquid velocity whereas it tends to decrease with increasing gas velocity. As shown in figure 3, the RMS values of the film thickness vary with both superficial liquid and gas velocities. It is evident that by increasing gas velocity this RMS value decreases, whereas it increases with liquid velocity. The effect of gas velocity appears to be comparatively stronger.

It should be pointed out that, in some of the following figures, data obtained by Paras *et al.* (1994) in a 50.8 mm i.d. horizontal pipe loop (in the stratified/atomization flow regime) are included to check for consistency and to examine general trends.

The mean large wave amplitude (dH) is found to be a linear function of the RMS value of the film height (figure 4); i.e. $dH = 2\sqrt{(2)}$ (RMS). This type of expression is representative of sinusoidal

Table 1. Summary of experimental conditions and results

Run	U_G (m/s)	U_L (m/s)	h_0 (mm)	dP/dx (N/m³)	Wetted wall fraction θ (degrees)	Liquid-to-wall shear stress at various circumferential positions, τ_{wL} (N/m²) 180°	157.5°	135°	112.5°	90°	67.5°	45°	22.5°	0°	315°	Upstream 45°
A	13.6	0.010	1.58	174.8	48	—	—	—	—	—	—	1.64	1.95	1.95	1.70	1.33
B	20.0	0.009	1.30	369.3	60	—	—	—	—	—	—	1.87	4.10	4.50	2.65	2.91
C	25.6	0.010	1.29	609.5	81	—	—	—	—	—	3.31	4.35	5.77	7.36	4.76	4.84
D	14.0	0.015	1.64	219.8	66	—	—	—	—	—	—	2.29	2.53	2.67	2.45	2.24
E	20.1	0.015	1.40	445.3	86	—	—	—	—	—	2.88	4.03	5.00	5.71	4.06	4.12
F	25.8	0.015	1.35	741.0	100	—	—	—	—	3.25	5.26	5.95	7.22	9.39	6.07	6.36
G	14.0	0.020	1.71	254.1	76	—	—	—	—	—	1.27	2.91	2.94	3.36	2.96	2.92
H	19.7	0.020	1.52	498.4	90	—	—	—	—	—	3.54	4.29	5.25	6.35	4.55	4.59
I	25.7	0.020	1.40	824.3	119	—	—	—	2.32	4.35	6.12	6.90	8.59	10.76	6.86	7.57
J	9.9	0.030	2.54	171.6	86	—	—	—	—	—	1.27	1.88	1.92	2.10	2.41	2.51
K	13.9	0.030	2.03	339.0	95	—	—	—	—	1.07	2.77	3.87	4.15	4.34	4.02	3.97
L	20.0	0.030	1.67	649.5	133	—	—	—	2.67	4.12	5.31	6.12	7.87	9.04	6.41	6.86
M	9.9	0.040	2.65	206.7	95	—	—	—	—	—	1.98	2.48	2.34	2.48	2.90	3.14
N	14.0	0.040	2.10	379.1	105	—	—	—	—	2.00	3.30	4.51	4.82	5.03	4.58	4.76
O	20.1	0.040	1.76	747.5	180	1.35	1.77	2.66	3.58	4.92	6.33	7.15	9.33	10.28	7.40	8.07
P	9.9	0.050	2.95	236.9	114	—	—	—	0.51	1.32	2.29	2.90	2.85	2.92	3.20	3.40
Q	14.0	0.050	2.31	419.1	180	0.50	0.64	0.81	1.69	2.55	3.57	5.01	5.19	5.53	4.97	5.34
R	20.0	0.050	1.89	827.6	180	1.52	2.53	3.38	4.58	5.99	7.01	8.15	10.49	11.80	8.42	9.26

wave motion and it seems to be applicable also in the case of irregular large waves encountered in the stratified/atomization flow regime. Paras and Karabelas (1991) reported that the above expression fitted quite well their data obtained in the annular flow regime. For relatively low superficial gas velocities, i.e. $U_G < 15$ m/s, large wave intermittency (I, defined as the fraction of total sampling time corresponding to passage of large waves) increases with gas velocity, whereas for U_G above 15 m/s it attains a value of about 0.3–0.4. Liquid flow rate seems to have no influence on the intermittency. Large wave height (h_w), sharply decreases with superficial gas velocity, but it is affected less by the liquid flow rate (figure 5). The aforementioned results are quite consistent with conclusions drawn by Paras *et al.* (1994), analyzing the same quantities. The approach followed for the determination of the large wave amplitude as well as its height and intermittency is presented in more detail by Paras and Karabelas (1991). In the latter study as well as in that

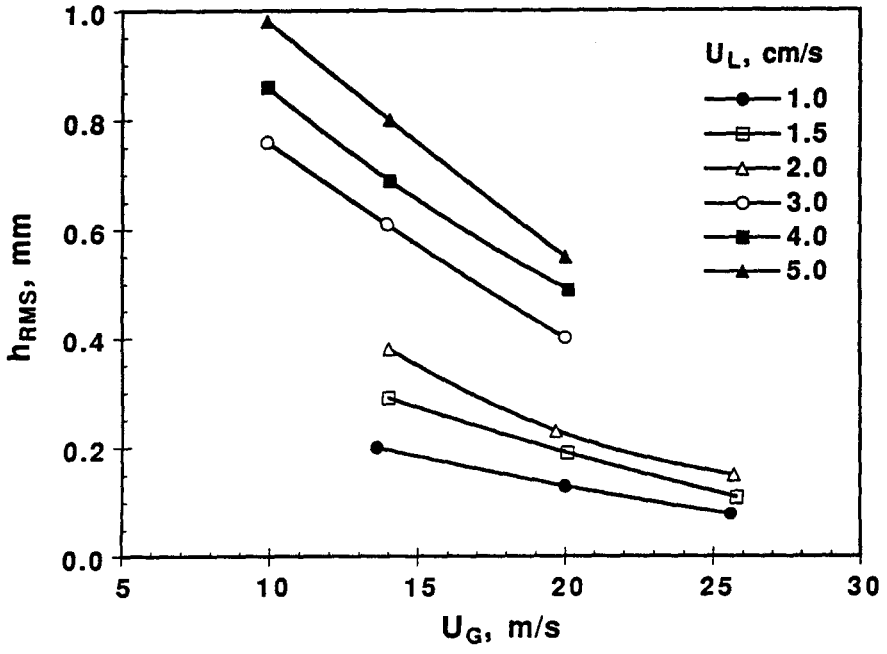

Figure 3. The effect of superficial gas and liquid velocities on film thickness RMS values at $\Theta = 0$ (i.e. pipe bottom).

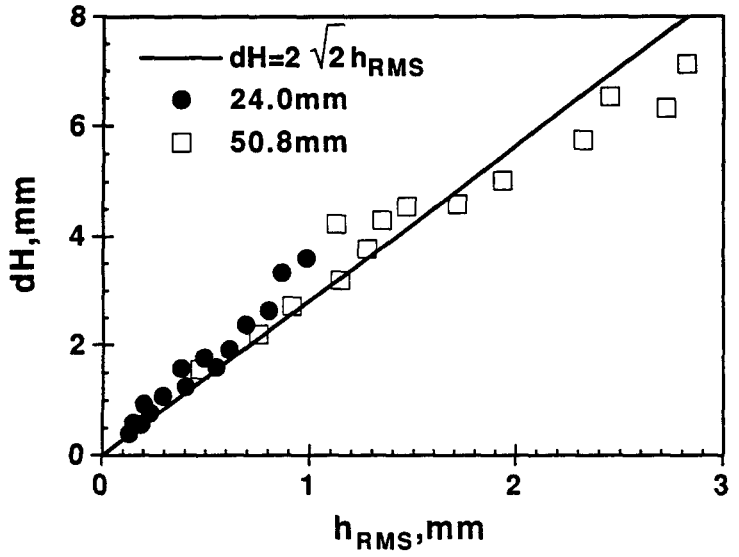

Figure 4. Correlation of large wave amplitude (dH) with film thickness RMS values at $\Theta = 0^\circ$ (i.e. pipe bottom). Data from 24 and 50.8 mm i.d. pipes.

of Hagiwara *et al.* (1995) experimental efforts are reported to describe the spatial arrangement of disturbance waves.

3.2. *Wetted wall fraction*

Hart *et al.* (1989) in their Apparent Rough Surface (ARS) model expressed the wetted wall fraction in terms of the angle θ. Later Grolman and Fortuin (1995) presented a Modified Apparent Rough Surface (MARS) model to extend it to cases of inclined flow. For the limiting case where the inclination angle is $\beta = 0^\circ$, their proposed correlation for the wetted wall fraction is close to that obtained from the ARS model. The predicted values of θ (from this model), for the test conditions of this work and for those of experiments conducted earlier by Paras *et al.* (1994), are

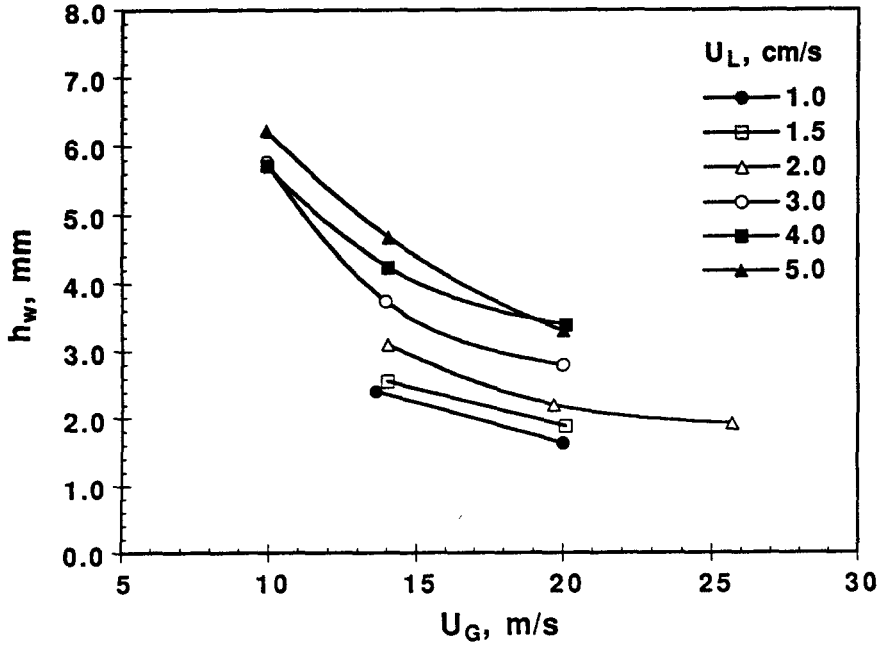

Figure 5. The effect of superficial gas and liquid velocities on large wave height (h_w) at $\Theta = 0^\circ$ (i.e. pipe bottom).

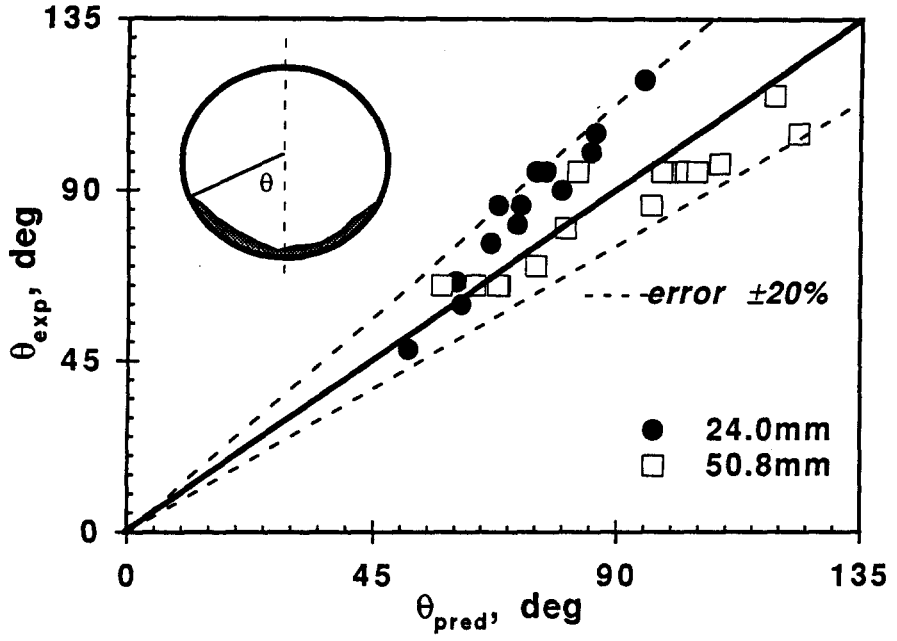

Figure 6. Wetted wall fraction data plotted against predicted values from the Hart *et al.* (1989) correlation.

in fairly good agreement (max deviation ~20%) with the observed ones, as shown in figure 6. A few runs corresponding to annular flow are obviously excluded from this figure.

As expected, and confirmed by visual observations, the area of the interface tends to increase with increasing gas velocity, and to deviate significantly from the flat (time-averaged) shape assumed in presently used computational procedures. It is also visually observed that the liquid film covering the lower part of the pipe circumference (although fairly thin) is continuous with no dry patches. Similar observations regarding the gas/liquid interface, were made by Paras *et al.* (1994) in their 50.8 mm i.d. horizontal loop, in the stratified/atomization flow regime.

3.3. Liquid-to-wall shear stress

As already mentioned, liquid-to-wall shear stress (τ_{wL}) was determined at various equidistant circumferential locations ($\Delta\Theta = 22.5^\circ$ intervals), using the well-known relation between the time-averaged diffusional current ($\bar{I}$) and the time-averaged velocity gradient ($\bar{S}$) at the probe surface

$$\bar{I} = 0.677 v_e F C_\infty D^{2/3} d^{5/3} \bar{S}^{1/3}, \quad [1]$$

where v_e is the number of electrons involved in the electrochemical reaction, F is the Faraday constant, C_∞ is the bulk concentration of the reacting species, D is the diffusivity of the ferricyanide ions, and, d is the circular probe diameter.

The value of τ_{wL} is obtained from the velocity gradient at the probe surface by Newton's law

$$\tau_{wL} = \mu_L \bar{S}, \quad [2]$$

where μ_L is the liquid viscosity.

It should be pointed out that [1] may not be valid for the *instantaneous* values of the diffusional current and the velocity gradient (but only for the time-averaged ones) unless a linear relation exists between these quantities. In the experiments reported here the intensity of fluctuating wall shear stress, T_s, defined as the ratio of root mean square (RMS) value of the wall stress over its mean value, is less than 0.35; i.e. relatively small. Under these conditions, the resulting average error from the use of instantaneous values in [1] (estimated to be 5%) is considerably smaller than the experimental errors associated with the electrochemical technique and with the determination (by calibration) of the actual probe diameter. It is noted that the maximum error may be as much as 20% if all the sources contribute in the same direction; this is however, unlikely as suggested also

by the following comparisons (figure 8). Rode *et al.* (1994) argue that the linear approximation is valid when the intensity of fluctuating diffusional current (T_i), defined as the ratio of the RMS value of the diffusional current fluctuations (i) over its mean value ($\bar{I}$), is less than 0.12. This linearity condition is satisfied in almost all the shear stress experiments conducted here.

Typical shear stress traces are shown in figure 7, for: (a) relatively low superficial gas velocity, i.e. for $U_G < 15$ m/s (run N) and (b) relatively high superficial gas velocity, i.e. for $U_G > 15$ m/s (run B). Time series, obtained at various lateral positions (for each run), were recorded simultaneously, under the same flow conditions. It is evident that these time records are very well correlated to each other and there is no time lag between them, as also confirmed by cross-correlation analysis. The peaks in these traces are attributed to gas/liquid interfacial waves which are also expected to influence flow conditions close to the pipe wall. In figure 8 time-averaged shear stress values obtained at 45°, for all runs, are compared to those obtained at 315°, at the same cross-section, and at 45°, at another cross-section 2 cm upstream from the former. The observed agreement gives additional credit to the electrochemical method employed here for making a reliable determination of the time-averaged local shear stress.

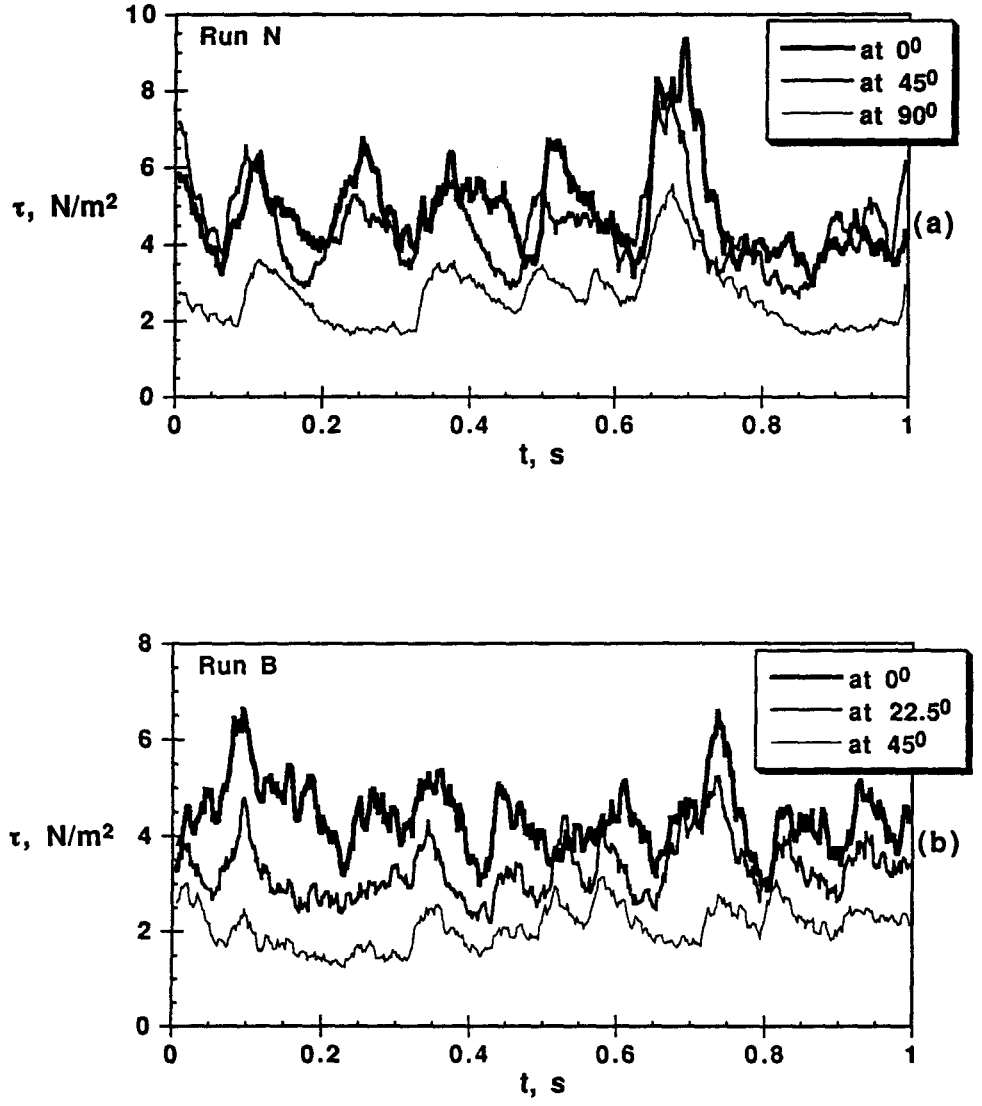

Figure 7. Typical traces of liquid-to-wall shear stress: (a) relatively low superficial gas velocity, i.e. $U_G < 15$ m/s; and (b) relatively high superficial gas velocity, i.e. $U_G > 15$ m/s.

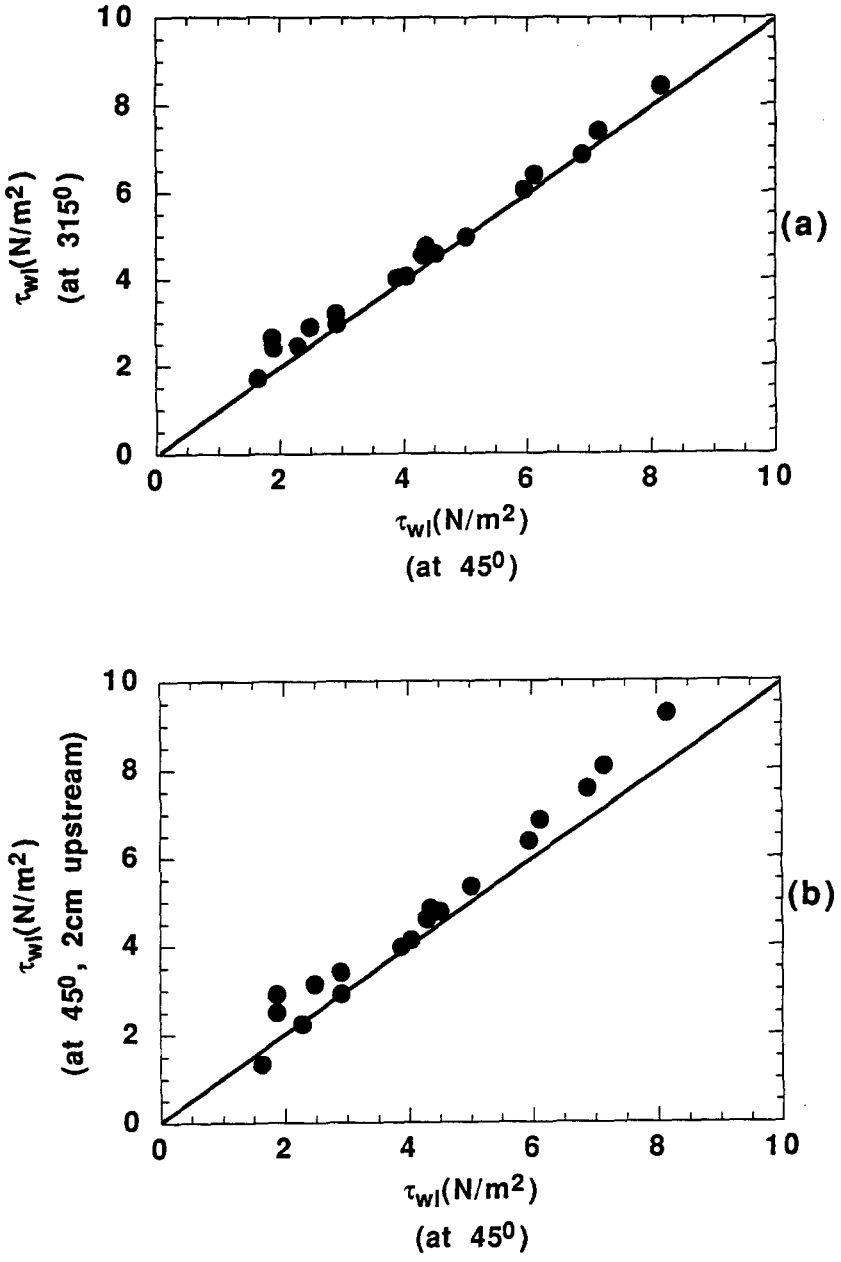

Figure 8. Time-averaged τ_{wL} at $\Theta = 45°$ plotted against: (a) τ_{wL} at $\Theta = 315°$, at the same cross-section; and (b) τ_{wL} at $\Theta = 45°$, at another cross-section 2 cm upstream.

Figure 9 shows typical spectra obtained at the pipe bottom (for the same run G) of: (a) film thickness, (b) shear stress, measured with the electrochemical technique and (c) shear stress, measured with hot-film anemometry. Paras *et al.* (1994) report that film thickness and shear stress power spectra display similarities which are indicative of the influence of waves on stress and on flow conditions at the wall. The same general conclusion is drawn from this figure; but regarding the shear stress spectrum in figure 9(b), it should be noticed that it exhibits only low characteristic frequencies (i.e. $f \approx 2$–3 Hz), whereas additional peaks in the high frequency part of the thickness spectrum (figure 9(a)) do not appear. The explanation possibly lies in the fact that the electrochemical mass transfer probes have a rather poor frequency response owing to the relatively small diffusion coefficient in liquids. Thus, a correction may be necessary by means of a frequency response transfer function, involving the ratio of fluctuations of the diffusional current and of wall shear stress (e.g. Nakoryakov *et al.* 1981; Nakoryakov *et al.* 1984; Deslouis *et al.* 1990; and Rode

et al. 1994). Since the emphasis here is placed on low frequencies, related to interface waves, no such correction is made. On the other hand, figure 9(c) shows that the shear stress spectrum, obtained with hot-film anemometry, is fairly similar to the film thickness spectrum even in the high frequency content. This may suggest that the frequency response of the hot-film probes is satisfactory as already reported in the literature. For example Fortuna and Hanratty (1971) state

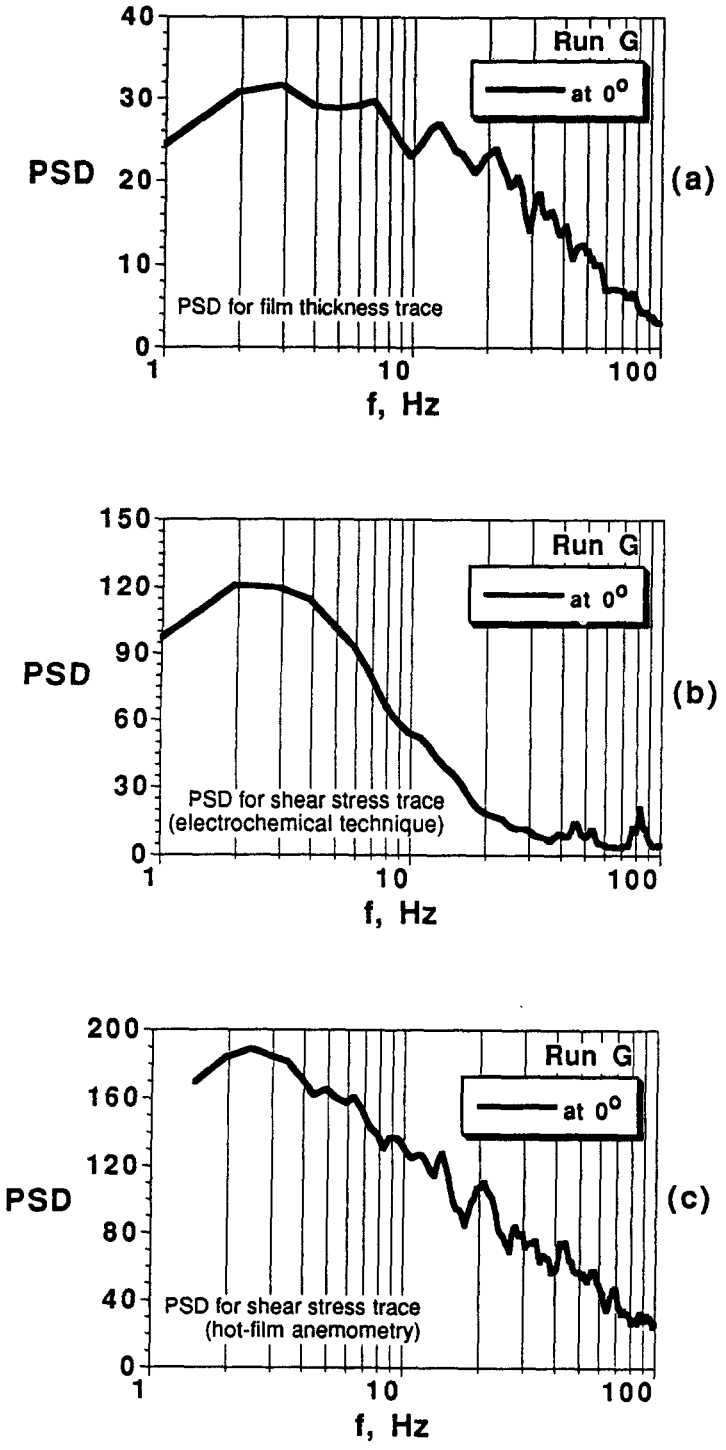

Figure 9. Typical spectra of: (a) film thickness; (b) shear stress, measured with the electrochemical technique; and (c) shear stress, measured with hot-film anemometry (run G).

that thermal probes have better frequency response than mass transfer probes on account of the different scalar boundary layer thickness influenced by the relatively small Prandtl ($Pr \approx 7$) and the large Schmidt number ($Sc \approx 3000$), respectively. Another advantage of the hot-film probe used in this work, as regards frequency response, is that the dimension of its sensing element in the streamwise direction is only 0.2 mm, as compared to the 0.5 mm diameter of the electrochemical probe, even though its overall diameter is much larger (~ 4 mm).

The time-averaged local shear stress is found to increase with both gas and liquid superficial velocities, at all radial positions. An inspection of table 1 reveals that for relatively low superficial gas velocities, i.e. for $U_G < 15$ m/s, the mean shear stress is roughly constant from $\Theta = 0°$ up to approx. 45°, where a fairly thick liquid layer is present; beyond that, it tends to decrease as the layer thickness tends to diminish circumferentially. For relatively high superficial gas velocities, i.e. for $U_G > 15$ m/s, where the film is observed to be very thin (except perhaps at the pipe bottom) the time-averaged shear stress obtains its maximum value again at $\Theta = 0°$ (i.e. at the pipe bottom), displaying a rather sharp reduction in the circumferential direction. These data are in qualitative agreement with those reported by Paras *et al.* (1994) in a 50.8 mm i.d. pipe, regarding the liquid-to-wall shear stress. It is pointed out that, contrary to these results, in the often quoted model of Taitel and Dukler (1976) the wall shear stress is arbitrarily assumed to be circumferentially constant. Fisher and Pearce (1979) also assume in their model, for describing horizontal annular flow, that τ_{wL} is uniformly distributed around the pipe circumference, although they find experimentally that time-averaged liquid-to-wall shear stress values tend to decrease laterally, away from the pipe bottom. Similarly, Rosant (1993) suggests (on the basis of local measurements) that, in horizontal and slightly downward flows, by increasing the gas velocity and developing a wavy interface, the lateral distribution of shear stress is roughly uniform, even though the scattering of his data is large. Finally, Krokovny *et al.* (1973) have taken measurements of wall shear stress circumferential distribution. Unfortunately, the way their data are reported does not allow one to directly compare them with the present measurements.

The following exponential expression is proposed, on the basis of the new data, to represent the aforementioned circumferential distribution of the axial liquid-to-wall shear stress τ_{wL}

$$\frac{\tau_{wL}(\Theta)}{\tau_{wG}} = 1 + \left(\frac{\tau_{wL0}}{\tau_{wG}} - 1\right)\left\{1 - \exp\left(-m\frac{\theta - \Theta}{\Theta}\right)\right\}, \qquad [3]$$

where τ_{wL0} is the liquid-to-wall shear stress at the pipe bottom ($\Theta = 0°$); θ is the wetted wall fraction; m is a fitting parameter. The quantity τ_{wG} is the gas-to-wall shear stress corresponding to gas velocity in the free cross section (defined by [10]). This quantity is considered to be constant, over the tube perimeter in contact with the gas phase (P_G), and equal to the liquid-to-wall shear stress value at the angle θ. As shown below, the τ_{wL} data clearly support this assertion. For the runs O, Q and R, observed to belong in the annular flow regime, τ_{wG} is replaced in [3] by the measured τ_{wL} value at 180° ($\theta = 180°$).

In the above mathematical form [3] the first derivative of the $\tau_{wL}(\Theta)$, at the bottom of the pipe ($\Theta = 0°$), equals zero—a condition dictated by symmetry. Integration of [3] from $\Theta = 0°$ to θ results in an average liquid-to-wall shear stress value, which may be very useful in modeling or other computational procedures. A similar formula, with two fitting parameters depending upon flow conditions, was proposed earlier by Sekoguchi *et al.* (1982), in order to correlate the film thickness circumferential distribution obtained in horizontal annular two-phase flow.

The parameter m in [3] was determined by usual regression methods and found to be strongly influenced by both gas and liquid superficial velocity; i.e. U_G and U_L, respectively. Thus, the calculated values of m were fitted quite well (figure 10) with the correlation

$$m = 70 U_G^{-2} U_L^{-0.4}. \qquad [4]$$

It should be pointed out that the applicability of this correlation was tested only for data obtained from the 24 mm i.d. pipeline.

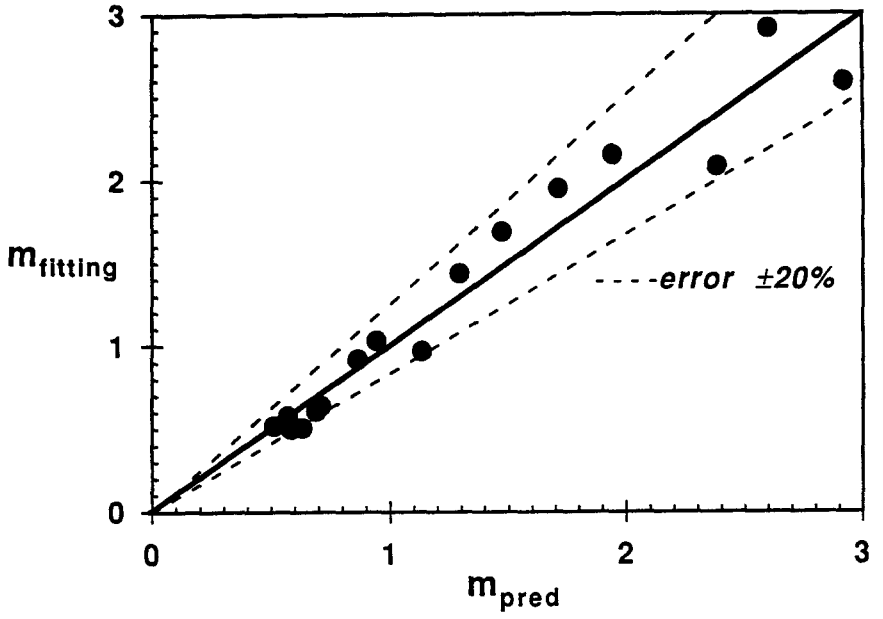

Figure 10. Fitting values of the parameter m vs predicted ones from [4].

The liquid-to-wall shear stress at the pipe bottom (τ_{wL0}) and the actual liquid velocity $U_{L,act}$ may be used to define a friction factor f_{L0}, so that:

$$\tau_{wL0} = f_{L0} \frac{\rho_L U_{L,act}^2}{2}, \quad [5]$$

where ρ_L is the liquid density and $U_{L,act} = U_L/\epsilon_L$ and ϵ_L is the liquid holdup.

Values of f_{L0}, obtained from [5], are fitted satisfactorily with a Blasius type equation

$$f_{L0} = 0.2 \mathrm{Re}_{LF}^{-0.25}, \quad [6]$$

where

$$\mathrm{Re}_{LF} = \frac{U_L h_0}{\epsilon_L \nu_L}$$

and h_0 is the time-averaged film thickness at the bottom of the pipe, and ν_L the liquid kinematic viscosity.

In figure 11 the experimental values of τ_{wL0}, for all runs, are plotted against the predicted ones using [5] and [6]. The maximum deviation is about $\pm 15\%$.

Thus, by employing [3]–[6] it is possible to determine the value of τ_{wL} at any lateral position around the pipe, if measurements are available of film thickness at the pipe bottom and of wetted wall fraction. If liquid holdup (ϵ_L) and wetted wall fraction (θ) data are not available, one may use [19] and [13] (for the holdup and the wetted wall fraction respectively), from the ARS model of Hart *et al.* (1989).

Figure 12 shows the circumferential distribution of $\tau_{wL}(\Theta)$ normalized, with respect to τ_{wG}, for: (a) run K with relatively low superficial gas velocity, where τ_{wL} is almost constant up to 45° (as previously mentioned), (b) run L with relatively high superficial gas velocity, where τ_{wL} is gradually reduced away from the pipe bottom and (c) run R, in the annular flow regime, which exhibits quite a similar behavior as run L of case (b). It will be noted that in figure 12(c) $\tau_{wL}(\Theta)$ is normalized with the measured τ_{wL} value at 180° ($\theta = 180°$). The lines drawn in this figure are based on [3]. In one line the experimental value of τ_{wL0} is used and the parameter m is obtained by best fit; in the other [4]–[6] are employed for calculating m and τ_{wL0}. For both lines, use is made of the visually obtained values for the wetted wall fraction (angle θ). The conclusion drawn here is that equations [3]–[6] allow successful matching of experimental shear stress data, obtained in this work at various lateral positions. Regarding the shear stress data obtained by Paras *et al.* (1994), the model

performs poorly in comparison with the experimental values at $\Theta = 0°$ (average error $\sim 30\%$), whereas the prediction for the shear stress values at $\Theta = 45°$ is more successful, with an average error less than 20%.

3.4. *Liquid-to-wall and gas/liquid friction factors*

The new data reported here on liquid-to-wall shear stress, at various locations around the pipe circumference, enable one to calculate more accurately an average value of τ_{wL}, using these measured values and the stress value at the angle θ. The latter was considered to be equal to the stress exerted by the gas flow on the solid wall (τ_{wG}). Thus, the liquid-to-wall friction factor f_L is computed from the corresponding average values of shear stress τ_{wL}. In figure 13 friction factor data (except those obtained in the annular flow regime) are plotted versus liquid Reynolds number Re_{LF}, based on actual liquid velocity and on mean film thickness at the pipe bottom, h_0. A quite satisfactory data correlation is obtained with the equation

$$f_L = 0.7 Re_{LF}^{-0.5}. \quad [7]$$

Kowalski (1987) using a Reynolds number based on superficial liquid velocity correlated his data with a similar expression, also involving a -0.5 exponent.

Averaged τ_{wL} data, obtained from measured values around the wetted portion of the pipe circumference, combined with data on liquid film thickness at the pipe bottom and pressure drop measurements, led to an improved determination of the interfacial friction factor, by means of momentum balances. For the computational procedure the gas/liquid interface was considered to be concave and not flat, as proved by visual studies.

The following equations were used, by employing momentum balances for the liquid and the gas phase, respectively

$$-A_L(dp/dx) - \tau_{wL}P_L + \tau_i S_i = 0, \quad [8]$$

$$-A_G(dp/dx) - \tau_{wG}P_G - \tau_i S_i = 0, \quad [9]$$

where the parameters A_L, A_G, P_L, P_G, S_i are defined in figure 14.These parameters are obtained from measured film thickness values at the pipe bottom, liquid hold-up values obtained by Hart *et al.* (1989)—their equation [19]—and the visual observations of wetted wall fraction (angle θ).

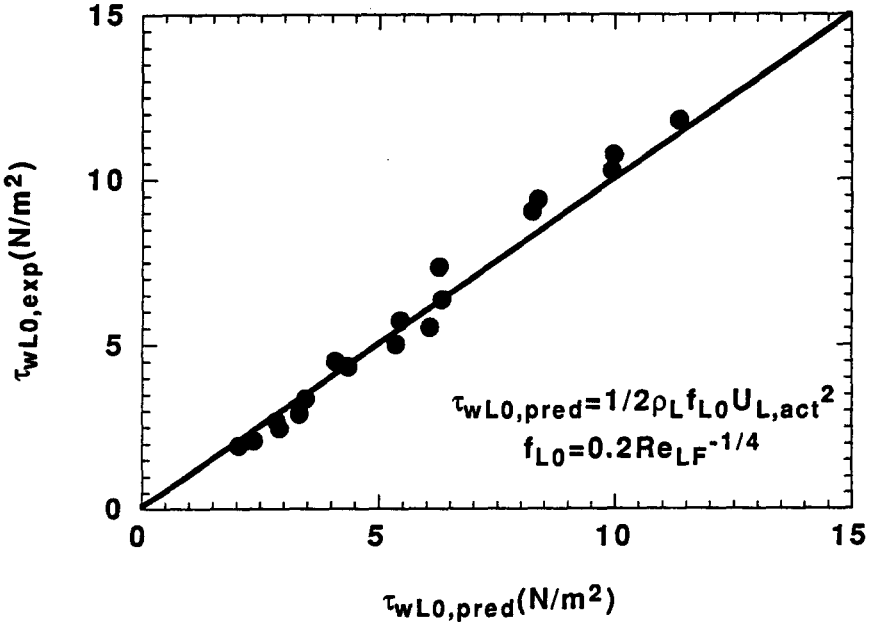

Figure 11. Experimental values of time-averaged τ_{wL0} (at $\Theta = 0°$, i.e. the pipe bottom) plotted against predicted values from [5] and [6].

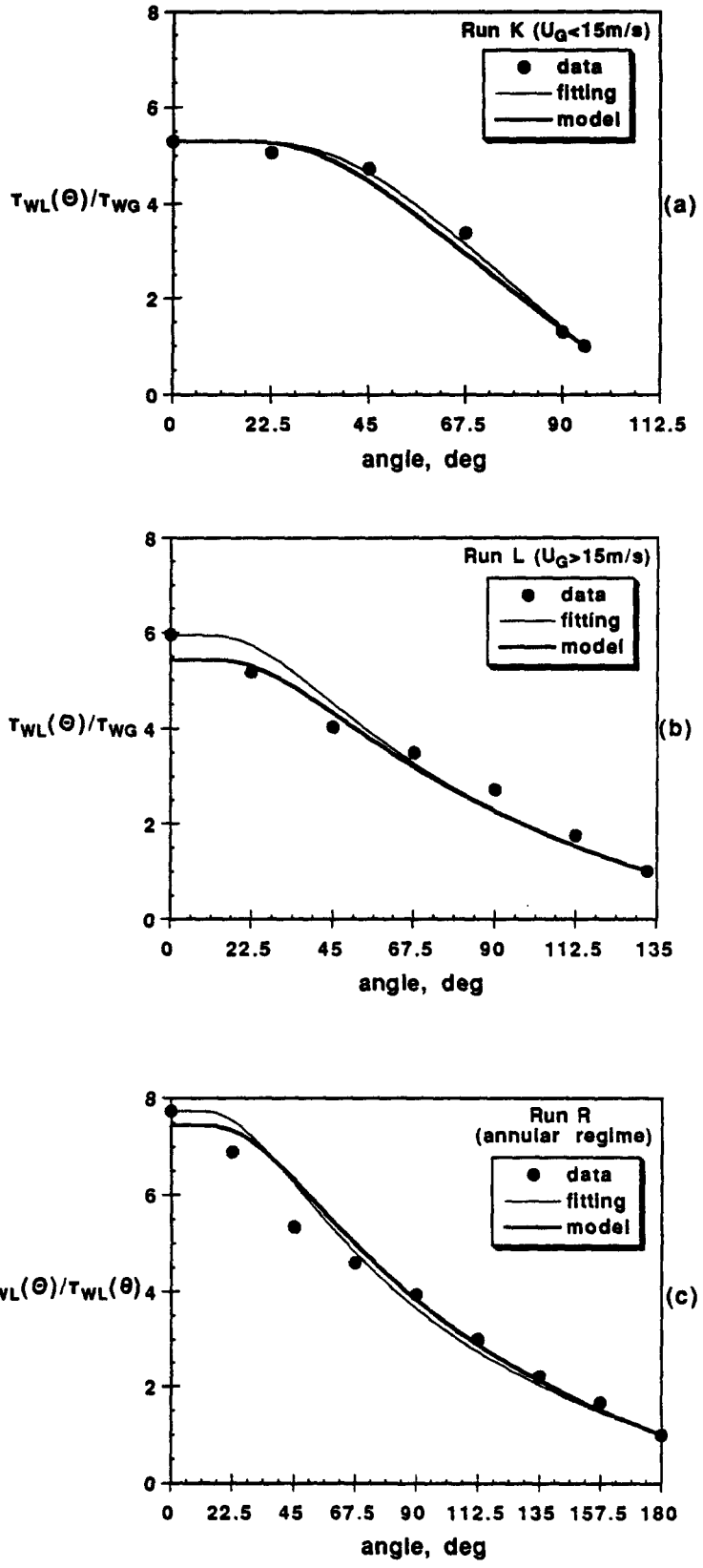

Figure 12. Circumferential distribution of τ_{wL} (Θ) normalized with respect to τ_{wG}: (a) relatively low superficial gas velocity, i.e. $U_G < 15$ m/s; (b) relatively high superficial gas velocity, i.e. $U_G > 15$ m/s; and (c) in the annular flow regime ($\tau_{wL}(\Theta)$ is normalized with respect to the measured τ_{wL} value at 180°).

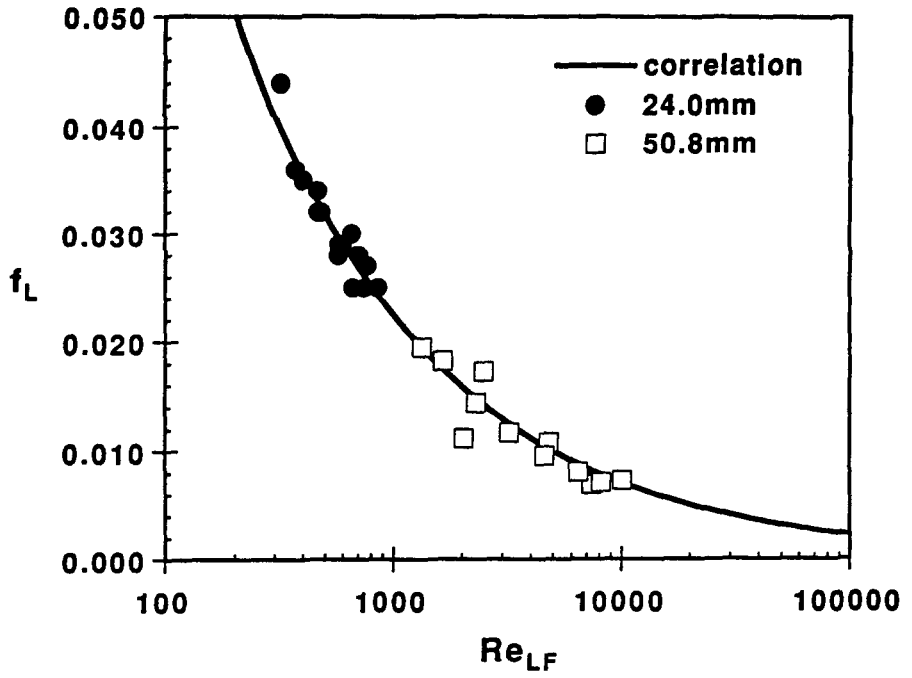

Figure 13. Liquid-to-wall friction factor (f_L) vs the Re_{LF} number.

The interfacial area S_i is approximated by taking the straight line segment CD instead of the arc CD (figure 14). The quantity $\tau_i \cdot S_i$ can be obtained from [8] using measured liquid film thickness, pressure drop (dP/dx) values, and the calculated average value of liquid-to-wall shear stress.

The gas-wall shear stress is calculated using a friction factor (f_G) and the superficial gas velocity (U_G); i.e.

$$\tau_{wG} = f_G \frac{\rho_G U_G^2}{2} \qquad [10]$$

with $f_G = 0.046 Re_G^{-0.2}$.

Therefore, the product $\tau_i \cdot S_i$ may be also computed using [9]. Very good agreement is obtained between the two values which differ only by 10%. Finally, an average value of the quantity $\tau_i \cdot S_i$

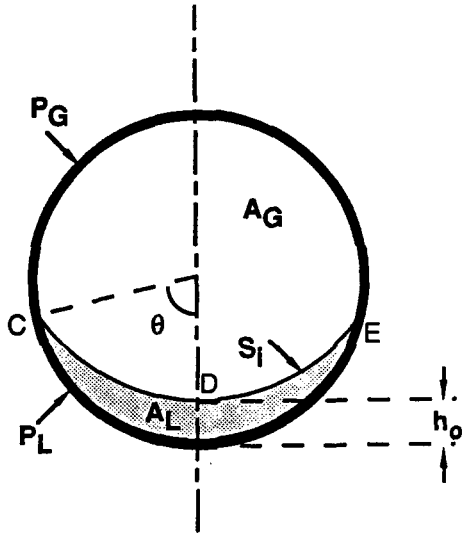

Figure 14. Representation of gas/liquid stratified/atomization horizontal flow.

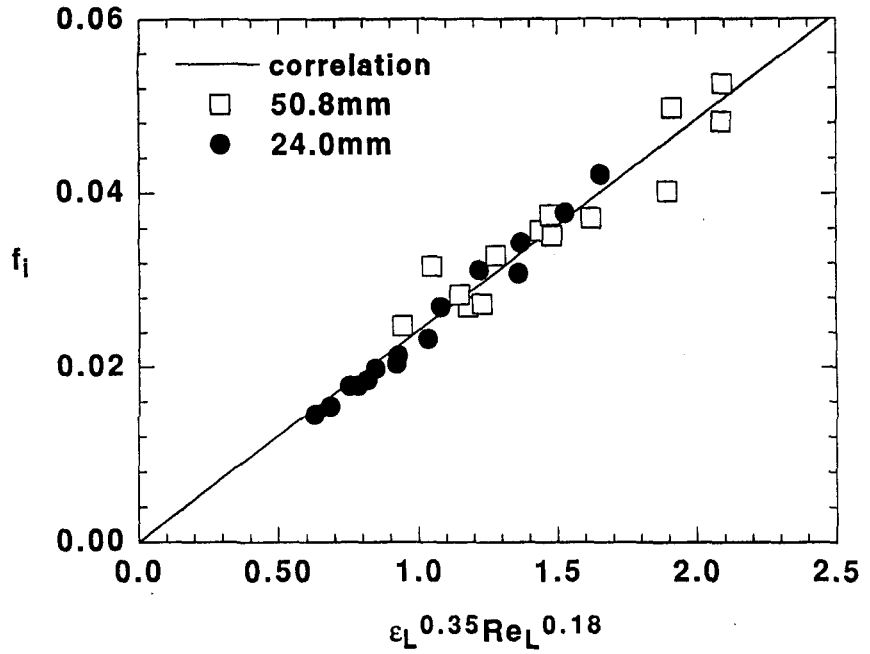

Figure 15. Correlation of gas/liquid interfacial friction factor (f_i).

is taken for evaluating the interfacial shear stress (τ_i). The latter is expressed in terms of an interfacial friction factor (f_i) and the superficial gas velocity (U_G)

$$\tau_i = f_i \frac{\rho_G U_G^2}{2}. \qquad [11]$$

Thus, the friction factor f_i is obtained, in the stratified/atomization flow regime, from [11] and found to be correlated quite well with the following expression, as shown in figure 15 (where f_i data obtained with the same procedure by Paras *et al.* (1994) are also plotted)

$$f_i = 0.024\epsilon_L^{0.35}\mathrm{Re}_L^{0.18}, \qquad [12]$$

where ϵ_L is the liquid holdup and Re_L the liquid Reynolds number, based on the superficial velocity and the pipe diameter. In order to estimate f_i, Kowalski (1987) proposed a similar power relation, based on liquid holdup and gas and liquid Reynolds numbers.

Another approach for calculating f_i is to consider the well-known resistance formula for the completely rough regime (Schlichting 1960)

$$f_i = \frac{0.25}{\left(2\log_{10}\frac{R}{k_s} + 1.74\right)^2} \qquad [13]$$

with R being the tube radius and k_s an apparent roughness.

Paras *et al.* (1994) determined an equivalent roughness for the gas/liquid interface by using independently obtained interfacial wave properties such as roll wave height, h_w, and intermittency, I. In the present work the calculated values of k_s, along with those obtained by Paras *et al.* (1994), normalized with respect to the pipe diameter, are fitted fairly well by the following correlation, as shown in figure 16 (where data obtained in the annular flow regime are excluded)

$$\frac{k_s}{D} = 2.85\left(\frac{dH}{D}\right)I^{0.17}. \qquad [14]$$

In the above expression the equivalent roughness is related to wave intermittency, I, and to wave amplitude, dH, instead of the wave height, h_w. The former is thought to represent more realistically,

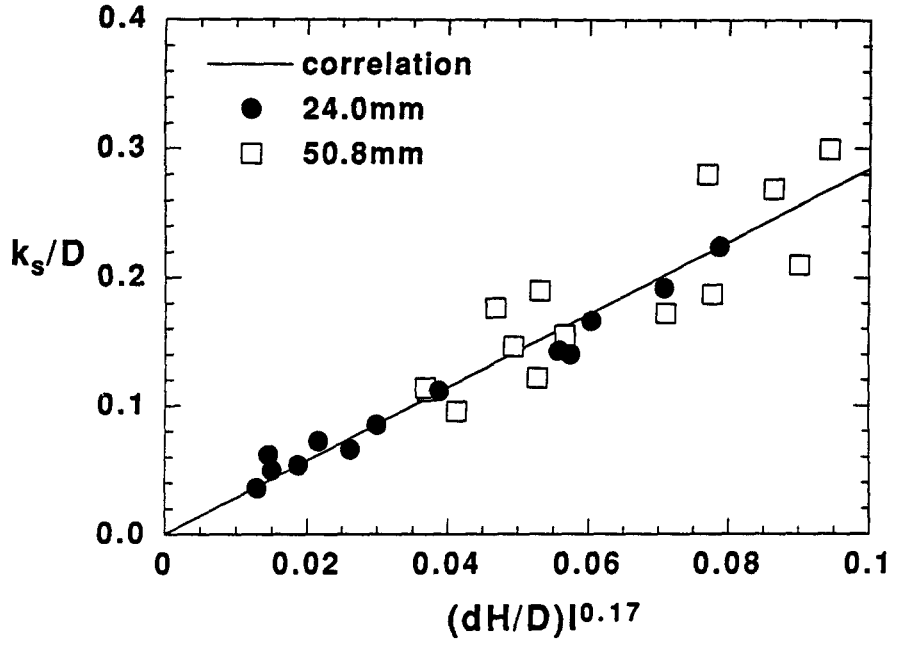

Figure 16. Apparent interface roughness (k_s) data correlated with large wave amplitude (dH) and intermittency (I).

than h_w, the actual height of the protrusions introduced by the waves into the gas flow. It should be pointed out that this correlation goes through zero as it would be required on physical grounds.

4. CONCLUDING REMARKS

At relatively small liquid flow rates, with low viscosity fluids such as those used in the present work, by increasing the gas velocity above 10 m/s the wavy stratified flow enters a transition regime, i.e. stratified/atomization. The main features of this regime are the presence of disturbance waves, with a characteristic frequency 1–15 Hz, the liquid droplets entrained in the gas phase, and the drastic change of the average gas/liquid interface profile from flat to concave.

In this work special attention is paid to the lateral distribution of the liquid-to-wall shear stress by making accurate measurements at various circumferential locations. Published information of this type, for highly asymmetric flows (such as stratified pipe flow), is rather limited, although it is considered essential for improving our physical understanding and for modeling. An important result regarding the time-averaged shear stress is that a significant lateral variation exists associated with the decreasing liquid film thickness, away from the bottom of the pipe. Only in the case of relatively low superficial velocities (i.e. $U_G < 15$ m/s), the mean shear stress is roughly constant up to $\Theta \approx 45°$, where a sufficiently thick liquid film exists. Beyond that lateral position, shear stress tends to decrease as the film thickness decreases to reach, at the angle θ of the triple-point (solid/gas/liquid), a value characteristic of the *gas*-to-wall shear stress. In an effort towards modeling this complicated flow regime, a generalized expression is proposed for predicting the shear stress lateral distribution. It will be pointed out, however, that this is a first attempt (based only on data taken by the authors) and that more measurements are required to test it and/or improve it, especially for large pipe diameters.

The observed reduction of liquid-to-wall shear stress with liquid film thickness, in the lateral direction, may be explained on the basis of a reduced (gas/liquid) interfacial shear in the same direction, caused by the lateral reduction of the wave height. Indeed, as has already been established (e.g. Paras and Karabelas 1991) the wave height tends to increase with liquid layer thickness.

By taking into account the correct shape of the gas/liquid interface and calculating with more accuracy (for each run) a liquid-to-wall shear stress, averaged over the wetted fraction of the pipe circumference, improved estimates of the interfacial friction factor f_i are obtained. For the model

calculations involving f_i, the film thickness, pressure drop and shear stress measurements are employed. Data on wave characteristics such as roll wave height (h_w), amplitude (dH) and intermittency (I) are computed and utilized in the analysis presented here. Finally an expression for an equivalent interface roughness is proposed.

Acknowledgements—Financial support by the Commission of European Communities under contracts JOUG-0005-C and JOU2-CT92-0108 is gratefully acknowledged.

REFERENCES

Agrawal, S. S., Gregory, G. A. and Govier, G. W. (1973) An analysis of horizontal stratified two phase flow in pipes. *Can. J. Chem. Eng.* **51,** 280–286.

Cognet, G., Lebouche, M. and Souhar, M. (1984) Wall shear measurements by electrochemical probe for gas–liquid two-phase flow in vertical duct. *AIChE J.* **30,** 338–341.

Deslouis, C., Gil, O. and Tribollet, B. (1990) Frequency response of electrochemical sensors to hydrodynamic fluctuations. *J. Fluid Mech.* **215,** 85–100.

Fisher, S. A. and Pearce, D. L. (1979) A theoretical model for describing horizontal annular flows. In *Two-phase Momentum, Heat and Mass transfer in Chemical, Process and Energy Engineering Systems*, Vol. 1, pp. 327–337. Durst, Tsiklauri & Afgan.

Fortuna, G. and Hanratty, T. J. (1971) Frequency response of the boundary layer on wall transfer probes. *Int. J. Heat Mass Transfer* **14,** 1499–1507.

Gordon, S. L., Newman, J. S. and Tobias, C. W. (1966) The role of ionic migration in electolytic mass transport: diffusivities of $[Fe(CN)_6]^{3-}$ and $[Fe(CN)_6]^{4-}$ in KOH and NaOH solutions. *Ber. Bunsenges. Phys. Chem.* **70,** 414–420.

Grolman, E. and Fortuin, J. M. H. (1995) The wavy-to-slug flow transition in inclined gas–liquid pipe flow. Presented at *Two-phase Flow Modelling and Experimentation*, Rome, Italy, pp. 1363–1370.

Hagiwara, Y., Esmaeilzadeh, E., Tsutsui, H. and Suzuki, K. (1989) Simultaneous measurement of liquid film thickness, wall shear stress and gas flow turbulence of horizontal wavy two-phase flow. *Int. J. Multiphase Flow* **15,** 421–431.

Hagiwara, Y., Yamaguchi, S. and Suzuki, K. (1995) Interfacial wave structure and its effect on transport phenomena in horizontal wavy/annular two-phase flows. *IUTAM Symp. on Waves in Liquid/Gas and Liquid/Vapour Two-phase Systems*, ed. S. Morioka and L. van Wijngaarden, pp. 257–267. Kluwer Academic Publishers, Netherlands.

Hart, J., Hamersma, P. J. and Fortuin, J. M. H. (1989) Correlations predicting frictional pressure drop and liquid holdup during horizontal gas–liquid pipe flow with a small liquid holdup. *Int. J. Multiphase Flow* **15,** 947–964.

Jolls, K. R. and Hanratty, T. J. (1969) Use of electrochemical techniques to study mass transfer rates and local skin friction to a sphere in a dumped bed. *AIChE J.* **15,** 199–205.

Karabelas, A. J., Wegner, T. H. and Hanratty, T. J. (1973). Flow pattern in a closed-packed cubic array of spheres near the critical Reynolds number. *Chem. Engng Sci.* **28,** 673–682.

Kowalski, J. E. (1987) Wall and interfacial shear stress in stratified flow in a horizontal pipe. *AIChE J.* **33,** 274–281.

Krokovny, P. M., Nakoryakov, V. E., Pokusayev, B. G. and Utovich, V. A. (1973) Experimental investigation of horizontal two-phase flow by an electrodiffusion method. *J. of Applied Mech. and Techn. Physics* **2,** 101–108.

McCready, M. J. and Hanratty, T. J. (1985) Effect of air shear on gas absorption by a liquid film. *AIChE J.* **31,** 2066–2074.

Miya, M., Woodmansee, D. E. and Hanratty, T. J. (1971) A model for roll waves in gas–liquid flow. *Chem. Engng Sci.* **26,** 1915–1931.

Nakoryakov, V. E., Kashinsky, O. N., Burdukov, A. P. and Odnoral, V. P. (1981) Local characteristics of upward gas–liquid flows. *Int. J. Multiphase Flow* **7,** 63–81.

Nakoryakov, V. E., Kashinsky, O. N. and Kozmenko, B. K. (1984) Electrochemical method for measuring turbulent characteristics of gas–liquid flows. In *Measuring Techniques in Gas–Liquid Two-phase Flows*, ed J. M. Delhaye and G. Cognet, pp. 695–721. Springer, Berlin.

Paras, S. V. and Karabelas, A. J. (1991) Properties of the liquid layer in horizontal annular flow. *Int. J. Multiphase Flow* **17,** 439–454.

Paras, S. V. and Karabelas, A. J. (1992) Measurements of local velocities inside thin liquid films in horizontal two-phase flow. *Experiments in Fluids* **13,** 190–198.

Paras, S. V., Vlachos, N. A. and Karabelas, A. J. (1994) Liquid layer characteristics in stratified-atomization flow. *Int. J. Multiphase Flow* **20,** 939–956.

Paras, S. V., Vlachos, N. A. and Karabelas, A. J. (1996) LDA measurements of local velocities inside the gas phase in horizontal stratified/atomization two-phase flow. Presented at *12th International Congress of Chemical and Process Engineering* (CHISA '96), Praha, Czech Republic.

Reiss, L. P. and Hanratty, T. J. (1962) Measurement of instantaneous rate of mass transfer to a small sink on a wall. *AIChE J.* **8,** 245–247.

Rode, S., Midoux, N., Latifi, M. A., Storck, A. and Saatdjian, E. (1994). Hydrodynamics of liquid flow in packed beds: an experimental study using electrochemical shear rate sensors. *Chem. Engng Sci.* **49,** 889–900.

Rosant, J. M. (1993) Liquid–wall shear stress in stratified liquid/gas flow. *Proc. of the 3rd Workshop International, Electrodiffusion Diagnostics of Flows*, Dourdan France, pp. 207–216.

Schlichting, H. (1960) *Boundary Layer Theory*, 4th edn. McGraw-Hill, New York.

Sekoguchi, K., Ousaka, A., Fukano, T. and Morimoto, T. (1982) Air–water annular two-phase flow in a horizontal tube. *Bulletin of the JSME* **25,** 1559–1566.

Selman, J. R. and Tobias, C. W. (1978) Mass-transfer measurements by the limiting-current technique. In *Advances in Chemical Engineering*, Vol. 10, pp. 211–318. Academic Press, New York.

Sobolík, V., Wein, O. and Cermák, J. (1987) Simultaneous measurement of film thickness and wall shear stress in wavy flow of non-Newtonian liquids. *Collection Czechoslovak Chem. Commun.* **52,** 913–928.

Taitel, Y. and Dukler, A. E. (1976) A model for predicting flow regime transitions in horizontal and near horizontal gas–liquid flow. *AIChE J.* **22,** 47–55.

Tsochatzidis, N. A. and Karabelas, A. J. (1994) Study of pulsing flow in a trickle bed using the electrodiffusion technique. *J. Appl. Electrochem.* **24,** 670–675.

Vogel, A. (1962) *Quantitative Inorganic Analysis*, pp. 371–372. Longmans, New York.

Zabaras, G. J. (1985) Studies of vertical annular gas–liquid flows. Ph.D. thesis, Univ. of Houston.